Protein-RNA Interactions in an Icosahedral Virus at 3.0 Å Resolution

ZHONGGUO CHEN, CYNTHIA STAUFFACHER, YUNGE LI, TIM SCHMIDT, WU BOMU, GREG KAMER, MICHAEL SHANKS, GEORGE LOMONOSSOFF, JOHN E. JOHNSON*

Nearly 20 percent of the packaged RNA in bean-pod mottle virus (BPMV) binds to the capsid interior in a symmetric fashion and is clearly visible in the electron density map. The RNA displaying icosahedral symmetry is single-stranded with well-defined polarity and stereochemical properties. Interactions with protein are dominated by nonbonding forces with few specific contacts. The tertiary and quaternary structures of the BPMV capsid proteins are similar to those observed in animal picornaviruses, supporting the close relation between plant comoviruses and animal picornaviruses established by previous biological studies.

COAT PROTEIN STRUCTURES OF SPHERICAL VIRUSES INFECTING mammals (*1–3*), insects (*4*), and plants (*5–7*) have been determined at near atomic resolution; however, protein–nucleic acid interactions in these viruses have been only indirectly suggested by disorder in portions of the protein subunits and by the distribution of basic residues on the interior surface of the capsid (*8*). Although regions of electron density have been assigned to RNA at low resolution (*9*), it has not been possible to construct detailed nucleic acid models in any spherical virus structure. We now report the structure of a virus particle in which about 20 percent of the packaged RNA is well ordered.

Using x-ray crystallography, we have investigated two members of the comovirus group, cowpea mosaic virus (CPMV) (*10*) and BPMV. CPMV is by far the most studied member of the comovirus group, but its properties have been shown to be general and apply to BPMV (*11, 12*). Comoviruses have a bipartite, positive sense, single-stranded RNA genome that is encapsulated with each RNA molecule in a separate particle (*13*). Empty capsids are also formed in vivo, and constitute approximately 20 percent of the particles in a typical preparation. Both RNA molecules of CPMV have been sequenced (*14, 15*). A portion of the small RNA (RNA2) of BPMV, which contains the coat protein genes, has been sequenced and the derived capsid protein sequences are reported below.

Comoviruses display a number of physical and biological properties that are similar to the animal picornaviruses (*13*). Although the genomic information is coded on a single RNA molecule in picornaviruses, the gene order of the two virus families is similar if the RNA's of CPMV are placed as is shown in Fig. 1 (*16*). RNA molecules of both comoviruses and picornaviruses are translated as polyproteins that are subsequently processed by two different proteases encoded in the viral genome (*17*). The capsids of both virus groups are composed of 180 β-barrel domains (Fig. 1) formed from three different protein types in picornaviruses (all approximately 30 kD) and two protein types in comoviruses (42 and 24 kD) (*1–3, 10*). Two electrophoretic forms of the whole particle have been found for comoviruses. In CPMV the small proteins of the fast electrophoretic form have a molecular size of about 20 kD while the small proteins in the slow form have the molecular size predicted by the sequence, 24 kD (*18*). Chemical analyses show that this difference in molecular size is due to the loss of 29 amino acids from the COOH-termini of the small proteins (*19*).

Structure determination. CPMV was propagated, purified, and crystallized in a cubic space group ($I23$, a = 317 Å) (*20, 21*). The 3.5 Å structure, as previously reported (*10*), was determined with crystals containing both nucleoprotein components. An electron density map at 3.0 Å resolution was subsequently calculated with an improved data set and polyalanine chains of both capsid subunits were traced in this map, but it was not possible to correlate the primary structure of the subunits with the distribution of side chain electron density.

BPMV was propagated, purified, and crystallized in an orthorhombic space group ($P22_12_1$, a = 311.2, b = 284.2, c = 350.5 Å) (*21*). The structure determination was done with crystals of virus particles containing only the small RNA (RNA2). Polyacrylamide gel electrophoresis (PAGE) analysis of dissolved crystals showed that only the cleaved ~20-kD form of the small protein was present, although a mixture of electrophoretic forms was in the solution used for crystallization. Photographic film data were collected from the orthorhombic crystals at the Cornell High Energy Synchrotron Source (λ = 1.566 Å). The data set of 182 A/B film pairs was scaled and postrefined (*22*) to produce 698,453 unique reflections where $I > 2\sigma(I)$ with an R_{merge} (*23*) of 9.6 percent. The final data set included nearly 90 percent of the complete data set between 20 and 3.0 Å resolution.

The $P22_12_1$ unit cell of the BPMV crystals contains two particles, and requires that one particle twofold symmetry axis be coincident with the lattice twofold axis **a**. Rotation functions (*24*), showed that the virus icosahedral twofold axes perpendicular to **a** were rotated 8.4 degrees from directional coincidence with the **b** and **c** twofold screw axes of the crystal lattice. Packing considerations indicated

Z. Chen, C. Stauffacher, Y. Li, T. Schmidt, W. Bomu, G. Kamer, and J. E. Johnson are in the Department of Biological Sciences, Purdue University, West Lafayette, Indiana 47907. M. Shanks and G. Lomonossoff are at the John Innes Institute, AFRC Institute of Plant Science Research, Colney Lane, Norwich NR4 7UH, United Kingdom.

*To whom correspondence should be addressed.

Table 1. Protein-RNA interactions. Potential hydrogen bonds between protein and RNA were based on interatomic distances of less than 3.6 Å. In each column the atom contributed by each chemical entity of the numbered nucleotide is indicated on the left, and the atom of the protein amino acids indicated on the right.

RNA	Phosphate	Ribose	Base
NA1			N2–Nη2 Arg^{3180} 2.70 Å
NA2			N2–Oε1 Glu^{3113} 3.56 Å
NA3		O2–O Thr^{3124} 3.37 Å	
		O2–N Ser^{3126} 3.41 Å	
NA4	O2P–Oγ Ser^{3126} 2.70 Å	03–Oγ Ser^{3126} 3.05 Å	
	O2P–Nζ Lys^{3073} 3.41 Å		
NA5	O2P–Oγ1 Thr^{4003} 2.70 Å		

that the only position for the virus particle center along the **a** axis that allows reasonable interparticle contact distances is near $x = 1/4$. The particle location was refined with the use of structure factors calculated to 8 Å resolution with the C_α coordinates of residues in the CPMV structure (*10*) positioned in the BPMV cell. Initial phases for BPMV were then calculated to 8 Å resolution from a properly positioned polyalanine model of CPMV. Extension of these phases to 3 Å resolution was done in steps, each step adding a volume of the reciprocal lattice equal to a shell of approximately two crystallographic indices in each direction (*25*). At each step the electron density map was averaged over the 30-fold noncrystallographic symmetry and an envelope was applied that had a 90 Å internal spherical radius and the exterior shape of the CPMV model. The α_{calc} from the back transform and F_{obs} with weights [the geometric mean of Sim and exponential weighting factors (*25*)] were used to compute a new electron density map. Structure factors not present in the measured data set were replaced with calculated amplitudes derived from the back-transformed map. The process was cycled at each resolution step until the average phase change was less than 5 degrees from the previous cycle. This process was continued to 3 Å resolution with a total of 40 extension steps and 121 cycles of averaging and Fourier transformation. The final molecular replacement R_{MR} (*26*) was 21.3 percent and the overall correlation coefficient C_{MR} (*27*) was .84 for 603,984 reflections. A model for the protein and RNA was built in the 3 Å electron density map, and the protein was refined according to the Hendrickson-Konnert procedure (*28*). After three rounds of refinement and rebuilding, the crystallographic R factor was 24 percent for data where $F > 5\sigma$ (F).

The sequences of the two coat proteins of BPMV were derived from complementary DNA (cDNA) clones of RNA2 (Fig. 2). Double-stranded cDNA to BPMV RNA2 was synthesized as described for red clover mottle virus RNA2 (*11*). The cDNA was digested with restriction enzymes, and the fragments were ligated with appropriately linearized bacteriophage M13 vectors. The resulting clones were sequenced by the dideoxy sequencing method (*29*), and the information was stored and assembled with the use of computer methods (*30*). More than 95 percent of the sequence covering the coat protein region of BPMV was obtained for both strands, and every base was sequenced at least twice.

Description of the BPMV structure. The two capsid proteins of BPMV are folded into three antiparallel β-barrel structures; the small protein forms one barrel and the large protein forms two barrels that are covalently connected to form a single polypeptide. The 60 copies of each protein type in the virus generate 180 β-barrel domains that are arranged in a manner very similar to a $T = 3$ capsid (Fig. 1). The gene order for the structural proteins in CPMV and poliovirus (Fig. 1) equates the large protein with VP2 and VP3, and the small protein with VP1, although there is no similarity in the primary sequences of these capsid proteins. The BPMV structure shows that the proteins equated by gene position also have equivalent positions in the capsid.

The primary and tertiary structures of the coat proteins of BPMV are shown in Fig. 2. The three domains that make up these proteins are wedge-shaped β-barrel units and are approximately 50 Å in length, 17 Å in width at the narrow end, and 30 Å at the wide end. Their thickness varies from 20 to 35 Å depending on the size of insertions between the β strands.

The C domain is the NH_2-terminal half of the large subunit and contains 182 amino acids, all of which are visible in the electron density map. This is the most helical of the domains, with each insertion between strands containing a well-defined α helix. The insertions are relatively short so that the main body of the β barrel (from the start of βB to the end of βI) is formed from only 150

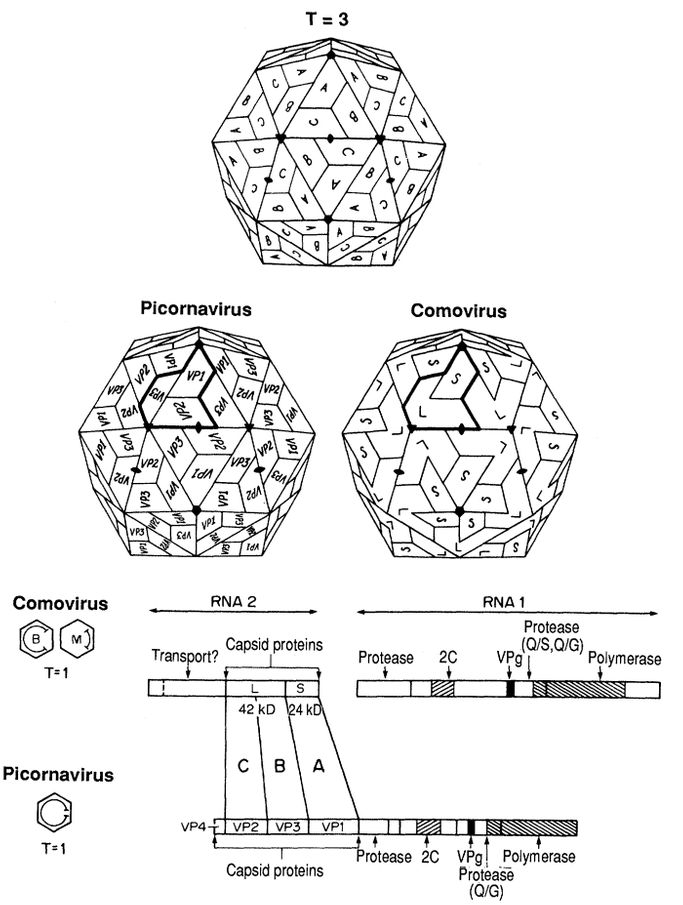

Fig. 1. A comparison of $T = 3$ picornavirus and comovirus capsids. In each case one trapezoid represents a β barrel. The icosahedral asymmetric unit of the $T = 3$ shell contains three identical subunits labeled A, B, and C. The asymmetric unit of the picornavirus capsid (in the heavy outline) contains three β barrels, but each has a characteristic amino acid sequence labeled VP1, VP2, and VP3. The comovirus capsid is similar to the picornavirus capsid except that two of the β barrels (corresponding to VP2 and VP3) are covalently linked to form a single polypeptide, the large protein subunit (L), while the small protein subunit (S) corresponds to VP1. Comoviruses and picornaviruses have a similar gene order, and the shaded regions of the nonstructural proteins display significant sequence homology. The relation between the subunit positions in these viruses and their location in the genes is indicated by the labels A, B, and C in the gene diagram.

residues compared to approximately 170 in domains A and B. The most unusual feature of this domain is the extended NH_2-terminal tail, which forms intersubunit contacts across the twofold axes on the interior surface of the virus capsid and interacts at its extreme end with the RNA.

The B domain is the COOH-terminal 192 residues of the large subunit. The β strands in this barrel have the largest twist of the three domains, giving it a very splayed appearance. The insertions, with the exception of the one between βC and βD, have little secondary structure. Two different routes for the last five residues at the COOH-terminus are found in the electron density for this domain. The one of stronger density extends to the front wall of the barrel (Fig. 2), but the route of lower occupancy stretches across the barrel toward the back wall and therefore is closer to the NH_2-terminus of the small subunit from which it is cleaved during capsid maturation (*13*). This less occupied conformation is 12 Å from the NH_2-terminus of the small protein, which implies a substantial rearrangement of portions of these two capsid proteins after the posttranslational cleavage.

The two wedge-shaped domains (C and B) of the large capsid protein lie side by side with the narrow ends together, packed around the virus threefold axes (Fig. 3). A 14-residue portion of the polypeptide chain connects the end of βI in domain C with the beginning of βB in domain B, defining one side of a shallow pocket on the inside of the capsid. The interface between these two domains is dominated by hydrophobic residues where polar or hydrophilic residues are usually found (*8*). These specific hydrophobic interactions may associate the two barrels into the side-by-side structure found in the virus particle as this subunit is synthesized.

The small subunit, which occupies the A position, is the most unusual of the barrels. It is a ten-stranded β barrel, since the βC–βD insertion forms two extra strands which lie on the top of the canonical barrel. The β sheets have an intermediate twist relative to the other domains, but the barrel is more streamlined to allow the tilted packing of this subunit around the fivefold axes. The conserved helix αA is raised relative to its position in the other domains. This shift in the tertiary structure is necessary to maintain similar interactions between the αA helices of the A and B domains as are seen in other intersubunit contacts. Consistent with the early chemical studies (*19*) and with the presence of a single electrophoretic form in the crystals, the 13 residues at the COOH-terminus of the small subunit were not visible in the electron density map. This subunit, like its counterpart VP1 in the picornaviruses, is also the most variable in primary structure when compared with other comovirus small subunit sequences (*31*).

The quaternary structure of the BPMV capsid gives the virus a nonspherical shape with characteristic large protrusions at the fivefold axes (Fig. 3). The large proteins, which by themselves form a perforated dodecahedron, are clustered around the threefold axes. The protrusions are formed by pentameric clusters of the small subunits around the fivefold axes. The general distribution of density in the capsid is similar to that found in the picornaviruses,

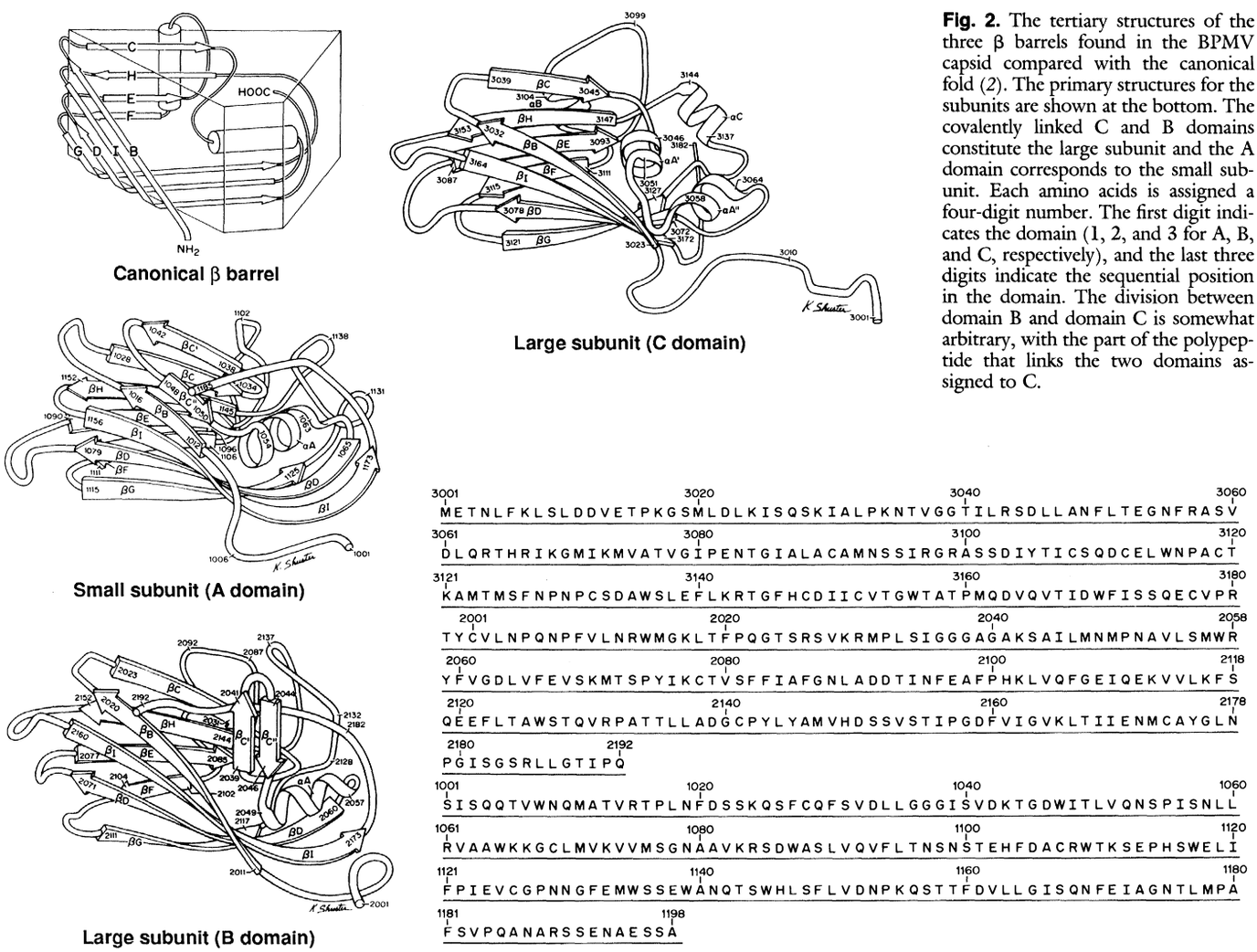

Fig. 2. The tertiary structures of the three β barrels found in the BPMV capsid compared with the canonical fold (*2*). The primary structures for the subunits are shown at the bottom. The covalently linked C and B domains constitute the large subunit and the A domain corresponds to the small subunit. Each amino acids is assigned a four-digit number. The first digit indicates the domain (1, 2, and 3 for A, B, and C, respectively), and the last three digits indicate the sequential position in the domain. The division between domain B and domain C is somewhat arbitrary, with the part of the polypeptide that links the two domains assigned to C.

```
3001                3020                3040                3060
METNLFKLSLDDVETPKGSMLDLKISQSKIALPKNTVGGTILRSDLLANFLTEGNFRASV
3061                3080                3100                3120
DLQRTHRIKGMIKMVATVGIPENTGIALACAMNSSIRGRASSDIYTICSQDCELWNPACT
3121                3140                3160                3180
KAMTMSFNPNPCSDAWSLEFLKRTGFHCDIICVTGWTATPMQDVQVTIDWFISSQECVPR
      2001                2020                2040                2058
TYCVLNPQNPFVLNRWMGKLTFPQGTSRSVKRMPLSIGGGAGAKSAILMNMPNAVLSMWR
      2060                2080                2100                2118
YFVGDLVFEVSKMTSPYIKCTVSFFIAFGNLADDTINFEAFPHKLVQFGEIQEKVVLKFS
      2120                2140                2160                2178
QEEFLTAWSTQVRPATTLLADGCPYLYAMVHDSSVSTIPGDFVIGVKLTIIENMCAYGLN
      2180          2192
PGISGSRLLGTIPQ
1001                1020                1040                1060
SISQQTVWNQMATVRTPLNFDSSKQSFCQFSVDLLGGGISVDKTGDWITLVQNSPISNLL
1061                1080                1100                1120
RVAAWKKGCLMVKVVMSGNAAVKRSDWASLVQVFLTNSNSTEHFDACRWTKSEPHSWELI
1121                1140                1160                1180
FPIEVCGPNNGFEMWSSEWANQTSWHLSFLVDNPKQSTTFDVLLGISQNFEIAGNTLMPA
1181          1198
FSVPQANARSSENAESSA
```

but the elaborate insertions between β strands that form part of the "canyon" receptor site and other surface features of the picornaviruses are absent in BPMV. The close fit between the large and small subunits shown within the heavy outline in the comovirus capsid in Fig. 3 suggests that this may be the protomer prior to cleavage. A similar grouping of subunits has been suggested as the precleavage protomer in picornaviruses (*1, 2*).

Protein-RNA interactions. Density comparable in height to that modeled as well-ordered protein, but not connected to any part of the polypeptide chain, was found inside the BPMV capsid. Seven ribonucleotides (labeled RNA1 to RNA7) were readily fitted to this density, which showed clear phosphate, sugar, and base densities and thus established the polarity of the chain (Fig. 4). The magnitude of this electron density implies that this portion of the RNA exists in virtually all of the 60 equivalent positions in the virus. The overall backbone stereochemistry of the seven ribonucleotide segment approximates that found in one strand of an A-type RNA helix. The average helical twist angle for the polyribonucleotide is 45 degrees while the mean rise per residue is 3.5 Å, so that the single strand of viral RNA is wound tighter than a strand in an A-type RNA helix, which has a twist angle of ~30 degrees and a rise per residue of 2.6 Å (*32*). The helical repeat distance for this RNA is roughly 28 Å, which is nearly the same as observed in the A-type helix. The viral RNA consists of eight residues per repeat and completes nearly one full turn in each ordered segment so that first the bases and then the phosphates face the protein.

The quality of the electron density for the bases was best at the 5′ end where the bases face the protein and weakens toward the 3′ end where they face the solvent in the virus interior. The density for each base represents an average of the different bases that must occur in the 60 asymmetric units of the virus. The bases of the entire segment of RNA are stacked. The density for the RNA1 and RNA2 positions is elongated and can accommodate purines, while the density for the RNA3 and RNA4 positions is more compact and is only large enough to accommodate pyrimidines. The orientation of the remaining bases is defined, but the density in which they are profiled is progressively smaller and is inadequate to accommodate even a pyrimidine.

The electron density for the seven-ribonucleotide segment is located near the icosahedral threefold axes. A tube of electron density about one-third the height of this well-ordered RNA density connects the 3′ terminal ribonucleotide of one of these segments to the 5′ terminal ribonucleotide of a threefold related segment. Four ribonucleotides (labeled RNA1′ to RNA4′) can be accommodated in this density, but the fit is ambiguous. Including these connecting ribonucleotides, the entire RNA forms a trefoil that consists of roughly 33 ribonucleotides surrounding each threefold icosahedral symmetry axis (Fig. 5). As viewed from outside the particle, the polarity of the chain goes from 5′ to 3′ in a clockwise direction. This cluster of 33 ribonucleotides may represent loops in the RNA secondary structure that recognize the threefold sites of the assembling virus. The detailed image of the RNA molecule entering and leaving the trefoils and the connections between the trefoils are not observed because they do not obey icosahedral symmetry. These "end effects" give rise to the weaker RNA density in the connecting regions because at most, only two of the three regions averaged can actually be present in any given trefoil. The total RNA modeled accounts for roughly 660 ribonucleotides (20 times 33) for the entire particle, which is about 20 percent of the packaged RNA.

A preliminary analysis of the environment of the RNA can be made on the basis of this map. The ordered ribonucleotides (RNA1 to RNA7) lie in a shallow pocket formed by the covalently linked C and B domains of the large subunit (Fig. 6). The surface of the pocket in which the RNA is located is formed by nine different segments of the capsid proteins which are rich in hydrophilic amino acids. Strands from the C domain β-barrel line the bottom of the pocket, with one side formed by the narrow end turns of the B domain β barrel and the other by the strand that connects the two domains. The 5′ to 3′ direction in the RNA runs antiparallel to the amino to carboxyl polypeptide direction of this connecting strand. The NH_2-terminal tail of a twofold related large protein closes the end of the pocket.

Most of the interactions between the RNA and protein are nonbonded electrostatic and van der Waals interactions although a few specific contacts may exist. All protein-RNA distances of less than 3.6 Å are listed in Table 1, although they cannot be specifically assigned as hydrogen bonds at this resolution. In addition, all but one of the polar side chains within 8 Å of the polynucleotide extend toward the polynucleotide chain. Interactions with these residues may be mediated by disordered polyamines or water molecules. The second RNA segment modeled in the electron density appearing at the lower contour level, makes no close contact with the capsid protein. Thus, in addition to the obligate disorder introduced by the end effects, this region is mobile because there are few stabilizing interactions.

Relation to other structures. The 3 Å resolution model of BPMV supports the close relation between comoviruses and picor-

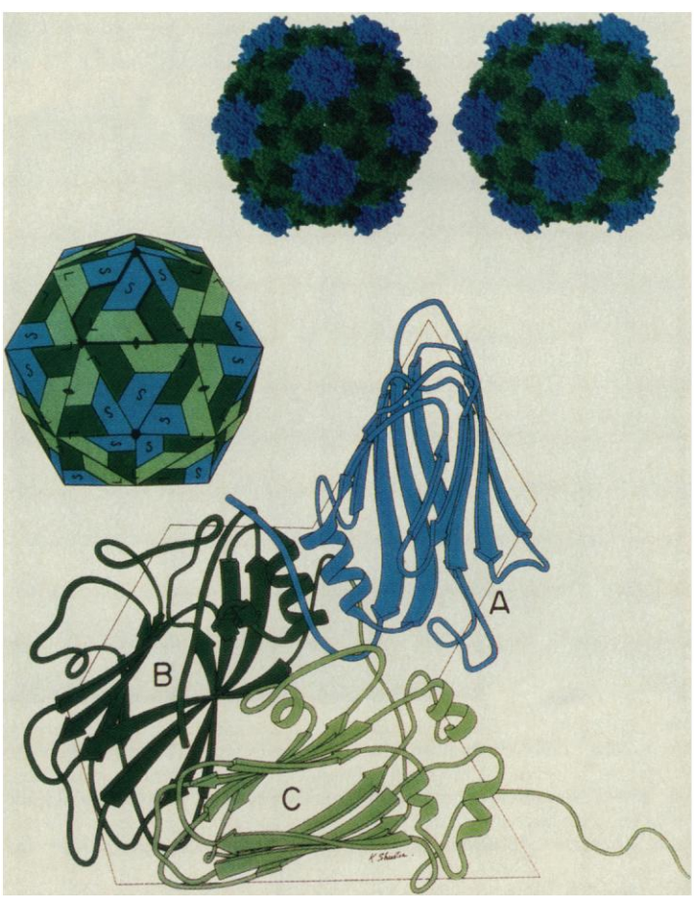

Fig. 3. The quaternary organization of the small and large subunits. The ribbon drawing represents the arrangement of the three β barrels in the virus quaternary structure. The two domains of the large subunit are shown in different shades of green to emphasize that they form one protein. The small subunit is shown in blue. The heavy outline in the capsid model encloses the suggested precleavage protomer. The stereoview of a space filling drawing of BPMV shows the large protrusions at the fivefold axes which extend 158 Å from the particle center.

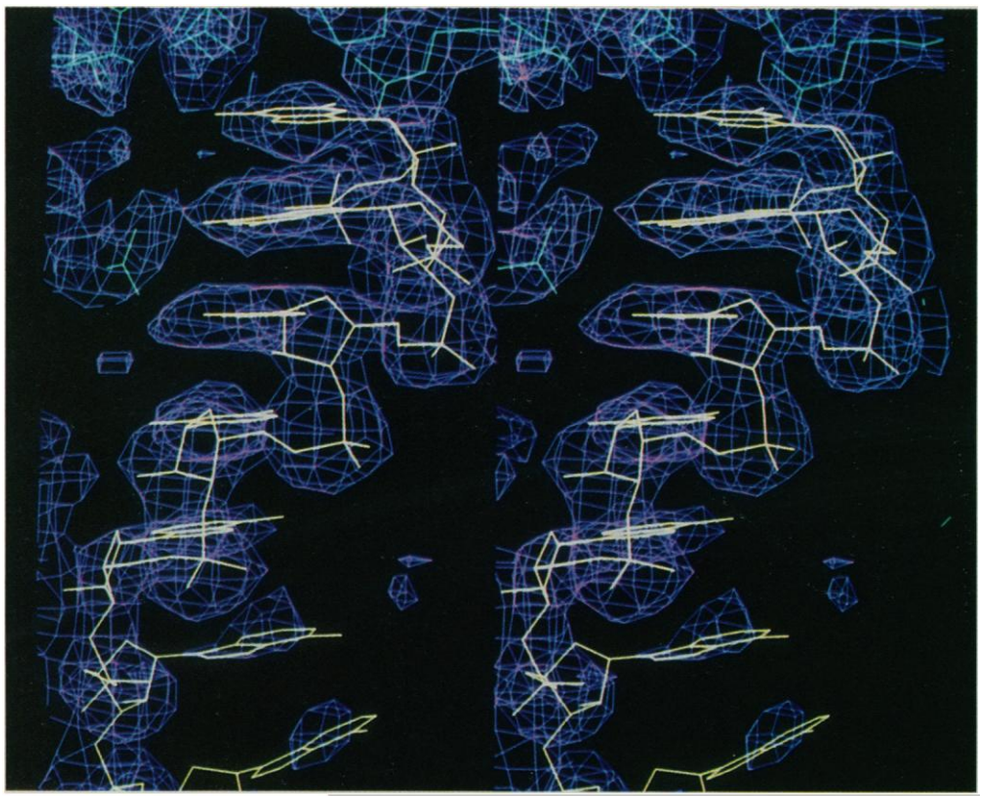

Fig. 4. A stereoview of the model of seven ribonucleotides, RNA1 (top) and RNA7 (bottom), superimposed on the electron density. As explained in the text, the density for the first two bases at the 5′ end (RNA1 and RNA2) are best fit by purines while the third and fourth are best fit by pyrimidines. The density for the last three bases is weak. The density displayed lies in a shell between 90 Å and 100 Å from the center of the virus just inside the protein shell.

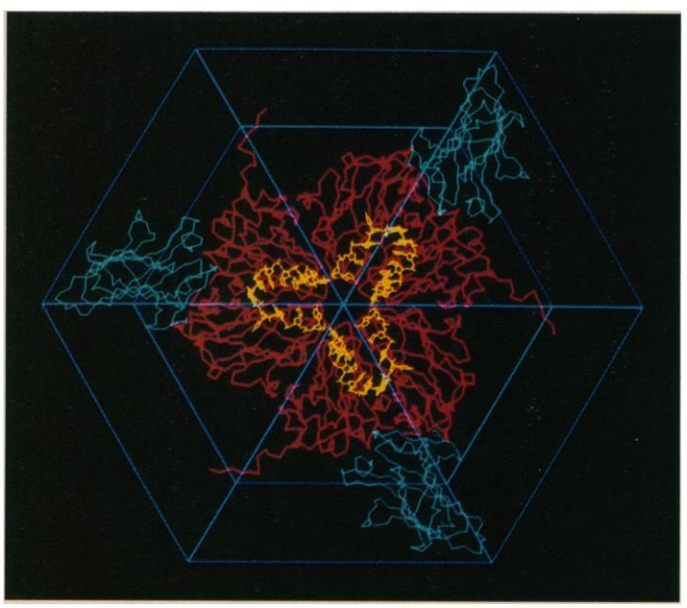

Fig. 5. The RNA (yellow) from three icosahedral asymmetric units forms a trefoil shape centered about the threefold particle axes. The large subunit is represented in red and the small subunit in blue; 33 ribonucleotides form this trefoil-shaped cluster, which appears connected in the electron density map but must have at least one point of entry and exit. Connections between these clusters of 33 ribonucleotides are not visible in the electron density map.

naviruses previously established by biological studies. Both viruses appear to have evolved from the more primitive $T = 3$ structure as a result of triplication of the gene coding for a β-barrel domain. The pseudo $T = 3$ capsid (Fig. 1) of picornaviruses containing three independent β barrels may provide a mechanism for rapid evolution in the presence of neutralizing antibody. A mutation in the coat protein of a $T = 3$ virus introduces changes in three locations in the icosahedral asymmetric structure unit; however, a similar mutation in a pseudo $T = 3$ capsid changes only one of the three β-barrel structures. This flexibility allows picornaviruses to escape immune surveillance more readily, a host pressure not exerted on plant viruses. Since comoviruses are the only confirmed example of pseudo $T = 3$ shells among the plant spherical viruses, a picorna-like ancestor of comoviruses may have passed from animals to plants through a common insect vector (*33*).

Previous high-resolution crystallographic studies of icosahedral viruses have not revealed any electron density attributable to RNA. In many of the simple spherical plant viruses and insect nodaviruses the RNA is bound to and neutralized by basic NH_2-terminal residues. These termini apparently are arranged in a variety of spatial positions that are dictated by the nucleic acid structure, thus rendering this portion of the protein, as well as the RNA, invisible in the electron density. In the comoviruses and picornaviruses polyamines, which are packaged in the particle, neutralize the RNA. Although three picornavirus structures have been reported (*1–3*), none have contained ordered RNA. Why are portions of the RNA visible in the BPMV structure and not visible in the similar picornavirus structures? There are several differences between BPMV and all other viruses of known three-dimensional structure: (i) Two different RNA molecules are encapsulated into separate particles with identical protein shells, (ii) comoviruses readily form empty capsids in vivo, and (iii) two of the β-barrel domains are formed by a single polypeptide. The first two of these observations suggest strong interactions between the coat protein subunits independent of the RNA. It is possible that the RNA is packaged when part of the capsid is already formed and is recognizing a preformed icosahedral environment. The connected β-barrel domains of the large subunit are part of this preformed environment. Like other simple spherical plant viruses, the NH_2-termini of both domains forming the large protein interact with the RNA. The covalent connection between the domains of the large subunit which forms one side of the RNA binding pocket is, in effect, the NH_2-terminus of the B domain. The NH_2-terminus of the C domain closes the end of the RNA binding pocket in a twofold related large subunit. This is the only terminus that extends any distance from a β-barrel domain and, like NH_2-termini in other viral subunits, it may be significant in the particle assembly and RNA packaging. These ordered positions for the NH_2-termini of the B and C domains may also contribute to the ordering of the RNA.

The BPMV structure shows the interaction of protein with a single-stranded, helical RNA. The high degree of RNA order is

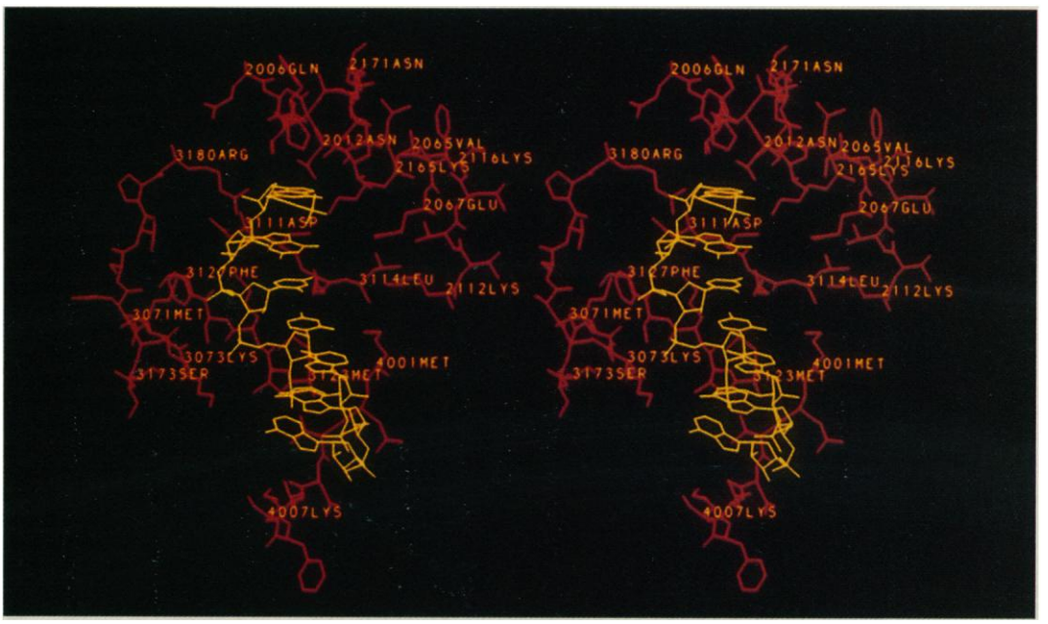

Fig. 6. A stereoview of the RNA (RNA1 to RNA7 from top to bottom) and the subunit side chains forming the hydrophilic pocket in which the RNA binds. Residues starting with 3 are in the C domain, those starting with 2 are in the B domain, and those starting with 4 are at the amino end of a twofold related C domain. The surface of the pocket is formed by nine different segments of the large subunit. Four segments lie in one C domain (3173–3180, 3071–3073, 3123–3127, and 3111–3114), one segment (4001–4007) lies in the twofold-related C domain, and four segments (2112–2116, 2065–2067, 2165–2167, and 2006–2012) are contributed by the B domain. The polypeptide segments 3175–3180, 3124–3127, and 4003–4004 follow almost the identical curvature as the sugar-phosphate backbone from RNA2-RNA6.

maintained by an electrostatic field and van der Waals interactions that exist within a hydrophilic pocket formed by the large protein. Analysis of the BPMV RNA sequence shows that the packaging is not dependent on an exactly repeating set of bases. Consistent with this observation, specific base interactions with the protein are limited. Likewise, the helical tobacco mosaic virus structure at 2.9 Å (*34*) shows few base specific interactions between protein and RNA, although a hydrogen bonding preference for GXX is suggested and is probably important in the assembly of the virus. In contrast to viral protein–nucleic acid interactions, regulatory proteins make much stronger sequence specific interactions with their cognate oligonucleotides (*35, 36*).

Many questions still exist about protein-RNA interactions in virus assembly, and BPMV is an excellent system to answer these questions. The structure of the empty capsid will show changes in the subunits that occur on binding RNA and the structure of the RNA1 containing virus component will show the effect of packaging a much larger RNA molecule in the same capsid.

REFERENCES AND NOTES

1. M. G. Rossmann *et al.*, *Nature* **317**, 145 (1985).
2. J. M. Hogle, M. Chow, D. J. Filman, *Science* **229**, 1358 (1985).
3. M. Luo *et al.*, *ibid.* **235**, 182 (1987).
4. M. V. Hosur *et al.*, *Proteins* **2**, 167 (1987).
5. S. C. Harrison, A. J. Olson, C. E. Schutt, F. K. Winkler, G. Bricogne, *Nature* **276**, 368 (1978).
6. C. Abad-Zapatero *et al.*, *ibid.* **286**, 33 (1980).
7. T. A. Jones and L. Liljas, *J. Mol. Biol.* **177**, 735 (1984).
8. M. G. Rossmann *et al.*, *ibid.* **166**, 73 (1983).
9. G. A. Bentley *et al.*, *ibid.* **194**, 129 (1987).
10. C. V. Stauffacher *et al.*, in *Crystallography in Molecular Biology*, D. Moras, J. Drenth, B. Strandberg, D. Suck, K. Wilson, Eds. (Plenum, New York, 1987), p. 293.
11. M. Shanks, J. Stanley, G. Lomonossoff, *Virology* **155**, 697 (1986).
12. R. I. B. Francki, R. G. Milne, T. Hatta, *Atlas of Plant Viruses* (CRC Press, Boca Raton, FL, 1985), vol. 2, pp. 1–16.
13. R. Goldbach and A. van Kammen, in *Molecular Plant Virology*, J. W. Davies, Ed. (CRC Press, Boca Raton, FL, 1985), p. 83.
14. P. Van Wezenbeek, J. Verver, J. Harmsen, P. Vos, A. van Kammen, *EMBO J.* **2**, 941 (1983).
15. G. Lomonossoff and M. Shanks, *ibid.*, p. 2253.
16. H. Franssen, J. Leunissen, R. Goldbach, G. Lomonossoff, D. Zimmern, *ibid.* **3**, 855 (1984).
17. H.-G. Krausslich and E. Wimmer, *Annu. Rev. Biochem.* **57**, 701 (1988).
18. T. J. Smith, *J. Virol. Methods* **16**, 263 (1987).
19. C. L. Niblett and J. S. Semancik, *Virology* **38**, 685 (1969).
20. J. M. White and J. E. Johnson, *ibid.* **101**, 319 (1980).
21. P. C. Sehnke *et al.*, *J. Crystal Growth* **90**, 222 (1988).
22. M. G. Rossmann, A. G. W. Leslie, S. S. Abdel-Meguid, T. Tsukihara, *J. Appl. Crystallogr.* **12**, 570 (1979).
23. $R_{merge} = \sum_h \sum_i | (F_h^2 - F_{hi}^2) | / \sum_h \sum_i F_h^2$
24. M. G. Rossmann and D. M. Blow, *Acta Crystallogr.* **15**, 24 (1962).
25. E. Arnold *et al.*, *ibid.* **A43**, 346 (1987).
26. $R_{MR} = \left(\sum_h |F_{h,obs} - F_{h,calc}| \right) / \sum_h F_{h,obs}$
27. $$C_{MR} = \frac{\sum_h (\langle F_o \rangle - |F_o(h)|) (\langle F_c \rangle - |F_c(h)|)}{\left(\sum_h (\langle F_o \rangle - |F_o(h)|)^2 (\langle F_c \rangle - |F_c(h)|)^2 \right)^{1/2}}$$
28. W. A. Hendrickson and J. H. Konnert, in *Computing in Crystallography*, R. Diamond, S. Ramaseshan, K. Venkatesan, Eds. (Indian Academy of Sciences, Bangalore, 1980), p. 13.01.
29. F. Sanger, S. Nicklen, A. R. Coulson, *Proc. Natl. Acad. Sci. U.S.A.* **74**, 5463 (1977).
30. R. Staden, *Nucleic Acids Res.* **8**, 3673 (1980).
31. A. C. Palmenberg, in *Molecular Aspects of Picornavirus Infection and Detection*, B. L. Semler and E. Ehrenfeld, Eds. (American Society for Microbiology, Washington, DC, in press).
32. S. Arnott, D. Hukins, D. Dover, W. Fuller, A. R. J. Hodgson, *J. Mol. Biol.* **81**, 107 (1973).
33. R. W. Goldbach, *Annu. Rev. Phytopathol.* **148**, 210 (1986).
34. K. Namba, R. Pallanyek, G. J. Stubbs, *J. Mol. Biol.*, in press.
35. S. R. Jordan and C. O. Pabo, *Science* **242**, 893 (1988).
36. A. K. Aggarwal, D. W. Rodgers, M. Drottar, M. Ptashne, S. C. Harrison, *ibid.*, p. 899.

37. Supported by NIH grant AI18764 (J.E.J.). Crystallographic computing on the graphics facility at Purdue University was supported by NSF grant DMB-85095449 (J.E.J.). We thank the staff of the Purdue University Computing Center for their help with computing on the Cyber 205; the staff at CHESS, Cornell University, Ithaca, NY, for assistance in crystallographic data collection; K. Shuster for preparation of the ribbon drawings, and S. Fateley for help in the preparation of the manuscript; P. Dumas, S. Krishnaswamy, and M. G. Rossmann for helpful discussions. In the United Kingdom, BPMV was handled under MAFF License Number PHF49A/85(17) in accordance with the Plant Pest's (Great Britain) Order 1980.

9 January 1989; accepted 26 May 1989